Journal of Physics and Chemistry of Solids 134 (2019) 64–68

Contents lists available at ScienceDirect

Journal of Physics and Chemistry of Solids

journal homepage: www.elsevier.com/locate/jpcs

One-step synthesis of high surface-area honeycomb graphene clusters for highly efficient capacitive deionization

Liang Chang, Yun Hang Hu*

Department of Materials Science and Engineering, Michigan Technological University, 1400 Townsend Drive, Houghton, MI 49931-1295, USA

ARTICLE INFO

Keywords:
Honeycomb graphene clusters
Capacitive deionization
Water treatment
Electrochemical double layers

ABSTRACT

Capacitive deionization (CDI) can realize ion adsorption efficiently by forming electrochemical double layers on electrode surfaces. This potential-driven adsorption process requires electrode materials possessing a large surface area as well as a rapid and easy electrolyte-diffusion pathway. In this respect, we designed and synthesized a novel honeycomb graphene cluster (HGC) based on one-step exothermic reaction between liquid lithium and carbon monoxide gas. The obtained HGC electrode, as both cathode and anode in a CDI cell, exhibited excellent desalination performance. Its electrosorption capacity reached 14.08 mg/g in a batch-mode system with continuously recycled 28 ml of 5 mM NaCl solution. This high-level desalination ability can be attributed to the effective utilization of HGC materials: its large surface area of up to 1962 m^2/g can provide abundant sites for ions adsorption, and three-dimensional mesoporous frameworks can facilitate ion transport. Thus, HGC electrodes can achieve electrosorption capacity of twice that of activated-carbon electrodes, indicating promising applications in the CDI field.

1. Introduction

Desalination of brackish water and seawater, which represent 97% of the available water supply on earth, can provide continuous and stable freshwater. This is a feasible solution for the freshwater crisis, and a powerful support for human consumption, residential life, agriculture, and industry development in the near future [1,2]. Currently, high energy consumption, high capital expenditure, and possible secondary pollution are the main drawbacks for conventional water desalination technologies (e.g. reverse osmosis and electrodialysis) [3–5]. To solve these issues, capacitive deionization (CDI), a novel desalination technology with energy-efficient and cost-effective features, has emerged and attracted much attention [6,7]. As a potential-driven process, CDI operates at 1–2 V applied potential and realizes desalination by an electrochemical double layer (EDL) mechanism [8]. As a result, deionized water is directly collected in the outlets of CDI cells and electrodes are regenerated by shorting the circuit and releasing absorbed ions back. Therefore, CDI (without high salinity limit, high membrane cost, and huge energy demand) is a promising water treatment technique [9].

The most important component of a CDI cell is the electrode. Its physical and structural properties greatly determine the desalination performance [10]. Activated carbon (AC), the commercially-used CDI electrode material, possesses surface areas up to thousands m^2/g but has limited electrosorption capacity due to inhibited ion transport in micropores [11,12]. This has stimulated us to design a high-performance CDI electrode material with a large surface area for ion adsorption, a continuous pathway for ion transport, and high electrical conductivity for small potential drop [13,14]. Effective strategies demonstrated in previous works include rational carbon polymorph, favorable morphology, suitable pore structure, and a functionalized surface by grafting and doping [15–19].

Graphene is a good choice for CDI electrode materials due to its intrinsic characters (high surface area and electrical conductivity) from single- or few-layer graphite structures [20]. The critical issue is that the severe aggregation of 2D graphene sheets induced by Van der Waals force can have a huge impact on electrosorption performance. Constructing a 3D structure for graphene materials can solve this issue and create novel characteristics. The interconnected porous structure not only buffers the volume changes during electrode preparation, but also provides pathways for ion transport. Additionally, the continuous framework formed by interlinked graphene sheets can achieve fast electron transfer [21,22]. Thus, ion adsorption capacity is significantly improved. Furthermore, we found that synthetic routes for 3D graphene (such as hydrothermal self-assembly, freeze-drying, self-sacrificial template synthesis, and chemical vapor deposition) can affect

* Corresponding author.
E-mail address: yunhangh@mtu.edu (Y.H. Hu).

https://doi.org/10.1016/j.jpcs.2019.05.040
Received 22 January 2019; Received in revised form 23 May 2019; Accepted 24 May 2019
Available online 26 May 2019

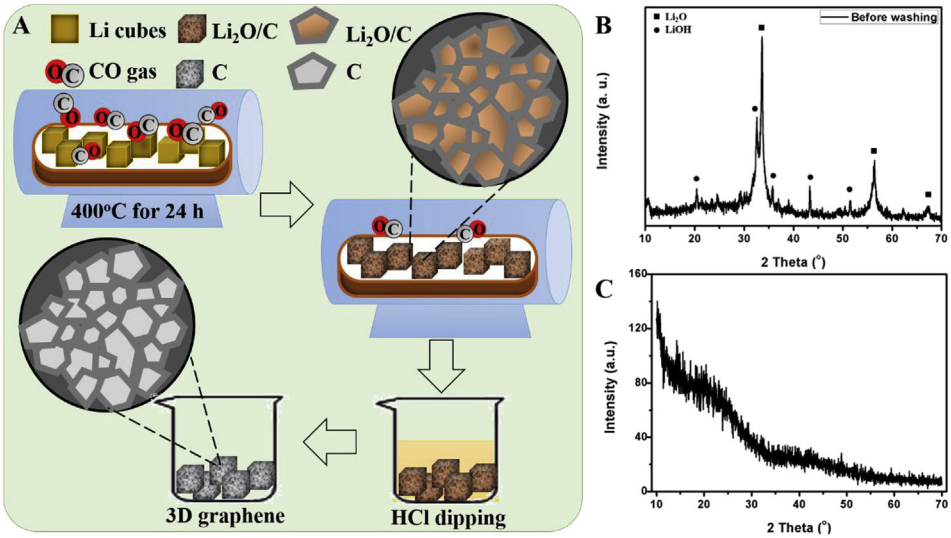

Fig. 1. (A) Schematic synthesis process of HGC, (B) XRD pattern of products before HCl treatment, and (C) XRD pattern of products after HCl treatment.

morphology, surface properties, and pore structure of products, corresponding with diverse electrochemical properties [23–26]. In recent years, our groups discovered numerous chemical reactions and applied them for the synthesis of high-quality 3D graphene with the expectation of mass production. These novel 3D carbon materials exhibited excellent performances for dye-sensitized solar cells, supercapacitors, and capacitive deionization [27–33]. In the present study, we explore novel honeycomb graphene clusters (HGC), successfully synthesized via our recently discovered reaction between lithium liquid and carbon monoxide gas, for CDI application. The HGC material possesses large surface areas of 1962 m^2/g and a three-dimensional porous framework, achieving high electrosorption capacity (14.08 mg/g) in a flow-through type CDI system. The obviously higher CDI performance of HGC, compared to AC, indicates it is an appropriate CDI material.

2. Results and discussion

Our recently discovered reaction between lithium liquid and carbon monoxide gas [34] was utilized to synthesize a 3D HGC (Fig. 1A). This reaction, with thermodynamic features of $\Delta H = -495.958$ kJ/mol and $\Delta G = -331.682$ kJ/mol, was operated in a batch ceramic reactor with temperature of 400 °C and time of 24 h. The X-ray diffraction (XRD) pattern and energy dispersive X-ray spectrometer (EDS) results confirm that the products are lithium oxide (Li_2O) and carbon. The presence of lithium hydroxide (Fig. 1B) may be attributed to Li_2O hydration in the atmosphere. Then, hydrochloride acid (HCl) treatment was conducted to remove the lithium compounds. As a result, graphene with amorphous structure is obtained as demonstrated by two wide diffraction peaks at 22.5° and 42.6° (Fig. 1C). The morphology of graphene was characterized by field emission scanning electron microscopy (FESEM). The coiled and bent graphene sheets grew along with simultaneously generated Li_2O nanoparticles, forming honeycomb clusters (Fig. 2A and B). The width of the honeycomb unit is estimated through transmission electron microscope image (TEM, Fig. 2C) as 30–50 nm. It well matches the size of Li_2O nanoparticles (about 39.7 nm) calculated from the Scherrer equation. Thus, this material is denoted as HGC.

The HGC was subjected to N_2 adsorption and desorption at liquid nitrogen temperature. A type-II N_2 adsorption/desorption isotherm is observed with a H3 hysteresis loop, implying a porous structure (Fig. S1A). Its large surface area of 1962 m^2/g was calculated with a BET model from the isotherm. Furthermore, HGC is a meso/macroporous material with large external surface area of 1758 m^2/g and main pore sizes of 5–10 and 40 nm (Fig. S1B). Furthermore, the surface properties of HGC were evaluated with Raman, EDS, X-ray photoelectron spectroscopy (XPS), and Fourier transform infrared spectroscopy (FTIR). The Raman spectrum (Fig. 2D) shows a D-band at 1350 cm^{-1} and a G-band at 1580 cm^{-1}, corresponding to disordered (sp^3 carbon) and ordered graphite (sp^2 carbon), respectively [23]. The intensity ratio of I_D/I_G is 1.08, indicating functional group modification on graphene sheets. The EDS measurement confirms that the HGC surface contains 9.1 wt% oxygen. The species of these oxygen functional groups are shown by XPS (Fig. 2E). The four deconvoluted peaks of C1s at 284.6, 285.9, 287.5, and 289.1 eV, correspond with C=C, O–C–O, C–O, and C=O, respectively [35]. Consistent results are shown by FTIR measurement. The IR bands at 1063, 1225, 1577, and 1720 cm^{-1} are associated with C–O, O–C–O, C=C, and C=O stretching vibration, respectively (Fig. 2F) [36]. The functionalized surface can not only contribute to a higher ion adsorption capacity but also benefit for wettability improvement. This is confirmed by dynamic contact angle measurement – good hydrophilicity of HGC is demonstrated by small advancing and receding contact angles of 44.6° and 33.1°, respectively (Figs. S2B and C).

These unique features mentioned above make HGC a potential candidate for CDI electrodes. Its electrochemical performance was evaluated using a three-electrode test cell with a HGC working electrode, a Pt foil counter electrode, and a saturated calomel reference electrode in 1 M NaCl aqueous solution. The cyclic voltammetry (CV) curve has a quasi-rectangular shape even at high rate (Fig. 3A), suggesting fast reversible adsorption and desorption of Na and Cl ions. Galvanostatic charge/discharge (GCD) with symmetrically triangular profiles further demonstrates this phenomenon (Fig. 3B). The excellent EDL property can be ascribed to four characteristics of HGC. (1) Its large surface area supplies abundant active sites for EDL formation. (2) Its mesoporous structure facilitates ion transport to the inner graphene surface at a high rate. (3) The three-dimensional continuous graphene framework provides fast electron transfer routes. (4) The modification of oxygen functional groups improves wettability of HGC and introduces additional pseudocapacitive adsorption.

To demonstrate the electrosorption capacity of HGC, a flow-type CDI cell with two identical HGC electrodes was fabricated for a batch-mode continuous circulation system as previously reported [31]. The feed solution of 28 ml of 5 mM NaCl aqueous solution was propelled by a peristatic pump. In the deionization process, a potential of 1.2 V was applied to the CDI cell for 30 min. The response current collected by electrochemical workstation exhibits a rapid drop in the initial potential and then approaches zero (Fig. 4A). The electrosorption capacity initially quickly increases and reaches a maximum of 5.52 mg/g with charge efficiency of 0.20 (Fig. 4B). Conversely, in the regeneration

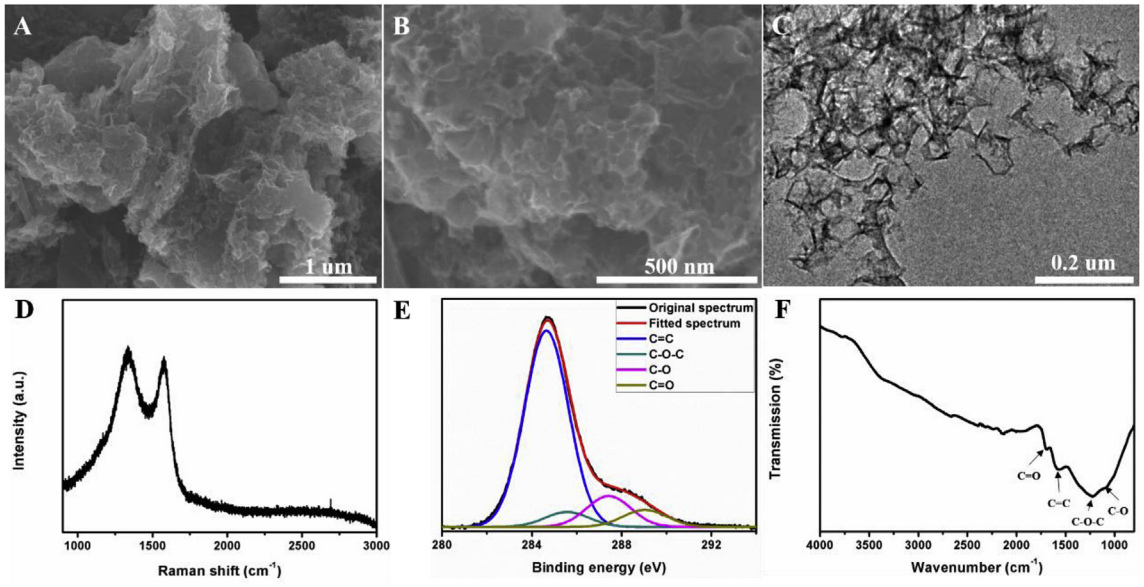

Fig. 2. Characterization of HGC: (A, B) SEM images, (C) TEM image, (D) Raman pattern, (E) XPS spectra, and (F) FTIR spectrum.

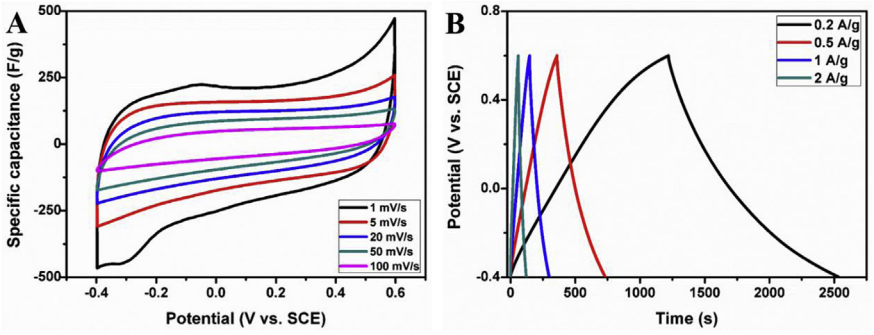

Fig. 3. Electrochemical performance of HGC electrodes with a three-electrode test cell in 1 M NaCl aqueous solution: (A) CV curves at scan rates of 1–100 mV/s and (B) galvanostatic charge/discharge profiles at current densities of 0.2–2 A/g.

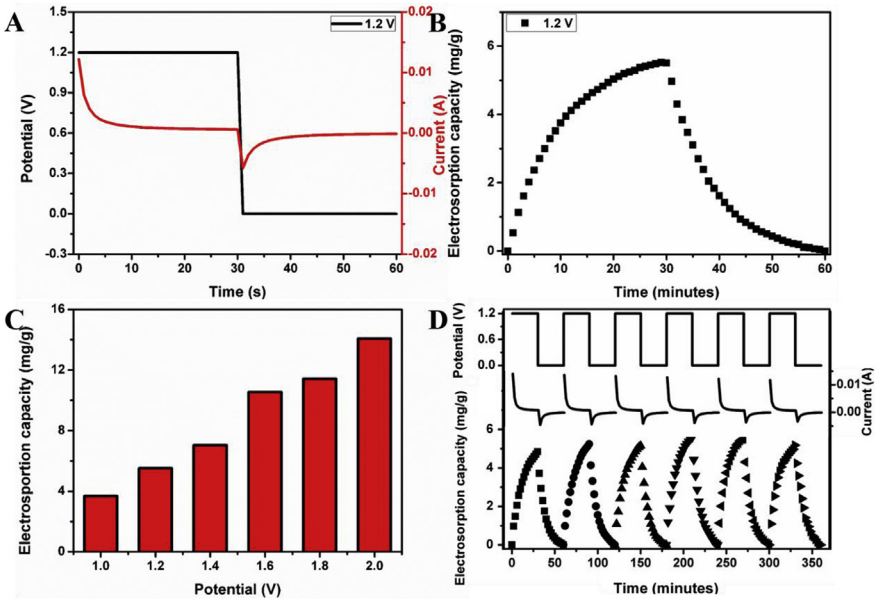

Fig. 4. Capacitive deionization performance of HGC in a batch-mode circulation system at flow rate of 10 ml/min (NaCl concentration of 5 mM): (A) applied potential and response current during a CDI cycle, (B) electrosorption capacity during a CDI cycle, (C) electrosorption capacities at different potentials, and (D) stability test for six cycles.

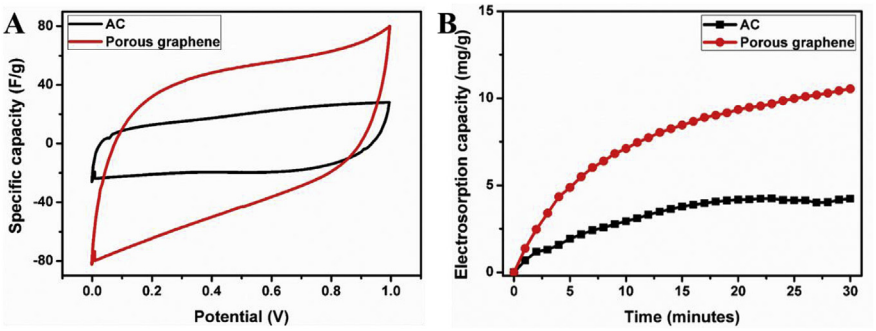

Fig. 5. Comparison between AC and HGC: (A) CV curves at scan rate of 5 mV/s with a two-electrode test cell in 5 mM NaCl solution and (B) electrosorption capacities at 1.6 V for 30 min with a flow-through CDI cell in a batch-mode configuration.

process, voltage is short circuited for another 30 min and the response current and electrosorption capacity both drop back to zero. The proportional relationship between electrosorption capacity and applied potential is shown in Fig. 4C. Namely, the electrosorption capacities of HGC electrodes increase along with potentials from 3.68, 5.52, 7.05, 7.51, 10.54, to 11.42 mg/g – maximum electrosorption capacity is achieved at 2.0 V, with 14.08 mg/g. Additionally, CDI Ragone plots show the electrosorption rate changes along with electrosorption capacity (Fig. S3). It is clear that the increased voltage enhances NaCl removal amount and rate, leading to right- and upper-shifted plots. Furthermore, the stability of HGC-based CDI cells was conducted at 1.2 V for 30 min of deionization and then at 0 V for 30 min of electrode regeneration (Fig. 4D). After six adsorption–desorption cycles, the electrosorption capacity is 5.3 mg/g, indicating good reversibility.

Finally, HGC and AC electrodes were compared under the same experimental conditions. The CV test with a two-electrode configuration was carried out at scan rate of 5 mV/s with potential range of 0–1 V in 5 mM NaCl. Both the HGC and AC electrodes show rectangular CV curves, suggesting good EDL effects (Fig. 5A). Obviously, the HGC electrodes with larger CV area possess higher adsorption ability and this is confirmed by a batch-mode flow-type CDI system. The HGC electrodes achieve electrosorption capacity of 10.54 mg/g with 30 min of ion adsorption at 1.6 V (Fig. 5B), larger than the 4.23 mg/g for AC electrodes. Thus, the HGC electrode is much better for CDI than the AC electrode.

3. Conclusion

Herein, a one-step exothermic reaction between lithium liquid and carbon monoxide was exploited to synthesize HGC. This had a three-dimensional graphene framework with 9% oxygen functional groups and a large surface area of 1962 m^2/g, which are favorable for EDL formation. As electrodes for CDI, HGC realized efficient ion removal from brackish water, leading to a large electrosorption capacity of up to 14.08 mg/g in a batch-mode flow-type CDI system. Such excellent performance can be attributed to the abundant active sites and continuous ion/electron transfer channels of HGC.

4. Experimental section

Detailed information on the experiments is provided in the Supplementary Materials. The following is a brief description of the experiments:

Synthesis of HGC: Lithium cubes (200 mg) were reacted with carbon monoxide gas (50 psi) in a batch-mode ceramic reactor at 400 °C for 24 h. Treatment of the collected products with 36.5 wt% HCl generated the HGC, which were characterized by various techniques, including XRD, FESEM, TEM, liquid-nitrogen-temperature N_2 adsorption–desorption isotherm, Raman and FTIR spectra, and XPS.

Electrode preparation and electrochemical/CDI performance of HGC electrodes: The HGC electrodes were prepared by casting homogenous slurry of 85 wt% HGC, 5 wt% carbon black, and 10 wt% poly(tetrafluoroethylene) on graphite foils. The HGC electrode can serve as a working electrode in a three-electrode test cell with Pt counter and saturated calomel reference electrodes or act as both cathode and anode in a two-electrode test cell. Both CV and GCD were utilized to examine the EDL properties. The CDI performance was tested in a batch-mode circulation system with peristatic pump control. A 273A Princeton potentiostat/galvanostat was used for control of applied potential and response current. A Horiba DS-71 conductivity meter equipped with a Horiba 3574-10C flow-type electrode determined the change of conductivity. The flow rate of feed water (28 ml of 5 mM NaCl aqueous solution) was 10 ml/min.

Author contributions

Y.H.H. designed material synthesis. L.C. synthesized and characterized materials and fabricated and evaluated capacitive deionization performance. Y.H.H and L.C. wrote the manuscript.

Declarations of interest

None.

Acknowledgements

U.S. National Science Foundation (CMMI-1661699) partially supported this work. The support of Charles and Carroll McArthur is also highly appreciated.

Appendix A. Supplementary data

Supplementary data to this article can be found online at https://doi.org/10.1016/j.jpcs.2019.05.040.

References

[1] E. Garcia-Quismondo, R. Gomez, F. Vaquero, A.L. Cudero, J. Palma, M. Anderson, New testing procedures of a capacitive deionization reactor, Phys. Chem. Chem. Phys. 15 (2013) 7648–7656.
[2] M.A. Ahmed, S. Tewari, Capacitive deionization: process, materials and state of the technology, J. Electroanal. Chem. 813 (2018) 178–192.
[3] E.N. Wang, R. Karnik, Graphene cleans up water, Nat. Nanotechnol. 7 (2012) 552–554.
[4] Z.H. Huang, Z. Yang, F. Kang, M. Inagaki, Carbon electrodes for capacitive deionization, J. Mater. Chem. A 5 (2017) 470–496.
[5] N. Pugazhenthiran, S.S. Gupta, A. Prabhath, M. Manikandan, J.R. Swathy, V.K. Raman, T. Pradeep, Cellulose derived graphenic fibers for capacitive desalination of brackish water, ACS Appl. Mater. Interfaces 7 (2015) 20156–20163.
[6] T. Kim, J. Yoon, CDI ragone plot as a functional tool to evaluate desalination performance in capacitive deionization, RSC Adv. 5 (2015) 1456–1461.
[7] P. Liu, T. Yan, L. Shi, H.S. Park, X. Chen, Z. Zhao, D. Zhang, Graphene-based materials for capacitive deionization, J. Mater. Chem. 5 (2017) 13907–13943.
[8] L. Chang, Y.H. Hu, Excellent capacitive deionization performance of meso-carbon

microbeads, RSC Adv. 6 (2016) 47285–47291.
[9] S. Porada, R. Zhao, A. van der Wal, V. Presser, P.M. Biesheuvel, Review on the science and technology of water desalination by capacitive deionization, Prog. Mater. Sci. 58 (2013) 1388–1442.
[10] Y.H. Teow, A.W. Mohammad, New generation nanomaterials for water desalination: a review, Desalination 451 (2019) 2–17.
[11] G. Wang, Q. Dong, Z. Ling, C. Pan, C. Yu, J. Qiu, Hierarchical activated carbon nanofibers webs with tuned structured fabricated by electrosorption for capacitive deionization, J. Mater. Chem. 22 (2012) 21819–21823.
[12] Y. Xu, L. Chang, Y.H. Hu, KOH-assisted microwave post-treatment of activated carbon for efficient symmetrical double-layer capacitors, Int. J. Energy Res. 41 (2017) 728–735.
[13] H. Yin, S. Zhao, J. Wan, H. Tang, L. Chang, L. He, H. Zhao, Y. Gao, Z. Tang, Three-dimensional graphene/metal oxide nanoparticle hybrids for high-performance capacitive deionization of saline water, Adv. Mater. 25 (2013) 6270–6276.
[14] C. Macias, G. Raines, P. Lavela, M.C. Zafra, J.L. Tirada, C.O. Ania, Mn-containing N-doped monolithic carbon aerogels with enhanced macroporosity as electrodes for capacitive deionization, ACS Sustain. Chem. Eng. 4 (2016) 2487–2494.
[15] P. Liu, T. Yan, J. Zhang, L. Shi, D. Zhang, Separation and recovery of heavy metal ions and salt ions from wastewater by 3D graphene-based asymmetric electrodes via capacitive deionization, J. Mater. Chem. A 5 (2017) 14748–14757.
[16] C. Zhao, G. Liu, N. Sun, X. Zhang, G. Wang, Y. Zhang, H. Zhang, H. Zhao, Biomass-derived N-doped porous carbon as electrode materials for Zn-air battery powered capacitive deionization, Chem. Eng. J. 334 (2018) 1270–1280.
[17] J. Han, L. Shi, T. Yan, J. Zhang, D. Zhang, Removal of ions from saline water using N, P co-doped 3D hierarchical carbon architectures via capacitive deionization, Environ. Sci. Nano 5 (2018) 2337–2345.
[18] J. Zhang, J. Fang, J. Han, T. Yan, L. Shi, D. Zhang, P. N, S co-doped hollow carbon polyhedral derived from MOF-based core shell nanocomposites for capacitive deionization, J. Mater. Chem. A 6 (2018) 15245–15252.
[19] X. Xu, H. Tan, Z. Wang, C. Wang, L. Pan, Y.V. Kaneti, T. Yang, Y. Yamauchi, Extraordinary capacitive deionization performance of highly-ordered mesoporous carbon nano-polyhedra for brackish water desalination, Environ. Sci. Nano (2019), https://doi.org/10.1039/C9EN00017H.
[20] H. Li, T. Lu, L. Pan, Y. Zhang, Z. Sun, Electrosorption behavior of graphene in NaCl solution, J. Mater. Chem. 19 (2009) 6773–6779.
[21] X. Xu, Z. Sun, D.H.C. Chua, L. Pan, Novel nitrogen doped graphene sponge with ultrahigh capacitive deionization performance, Sci. Rep. 5 (2015) 11225.
[22] A. Amiri, G. Ahmadi, M. Shanbedi, M. Savari, S.N. Kazi, B.T. Chew, Microwave-assisted synthesis of highly-crumpled, few layered graphene and nitrogen-doped graphene for use as high-performance electrodes in capacitive deionization, Sci. Rep. 5 (2015) 17503.
[23] Z.Y. Yang, L.J. Jin, G.Q. Lu, Q.Q. Xiao, Y.X. Zhang, L. Jing, X.X. Zhang, Y.M. Yan, K.N. Sun, Sponge-templated preparation of high surface area graphene with ultra-high capacitive deionization performance, Adv. Funct. Mater. 24 (2014) 3917–3925.
[24] X. Xu, L. Pan, Y. Liu, T. Lu, Z. Sun, D.H.C. Chua, Facile synthesis of novel graphene sponge for high performance capacitive deionization, Sci. Rep. 5 (2015) 8458.
[25] W. Shi, H. Li, X. Cao, Z.Y. Leong, J. Zhang, T. Chen, H. Zhang, H.Y. Yang, Ultrahigh performance of novel capacitive deionization electrodes based on a three-dimensional graphene architecture with nanopores, Sci. Rep. 6 (2016) 18966.
[26] X. Cao, Y. Shi, W. Shi, G. Lu, X. Huang, Q. Yan, Q. Zhang, H. Zhang, Preparation of novel 3D graphene networks for supercapacitor application, Small 7 (2011) 3163–3168.
[27] H. Wang, K. Sun, F. Tao, D.J. Stacchiola, Y.H. Hu, 3D Honeycomb-like structured graphene and its high efficiency as a counter-electrode catalyst for dye-sensitized solar cells, Angew. Chem. Int. Ed. 52 (2013) 9210–9214.
[28] L. Chang, W. Wei, K. Sun, Y.H. Hu, 3D flower-structured graphene from CO_2 for supercapacitors with ultrahigh areal capacitance at high current density, J. Mater. Chem. A 3 (2015) 10183–10187.
[29] L. Chang, D.J. Stacchiola, Y.H. Hu, Direct conversion of CO_2 to meso/macro-porous frameworks of surface-microporous graphene for efficient asymmetrical supercapacitors, J. Mater. Chem. A 5 (2017) 23252–23258.
[30] L. Chang, D.J. Stacchiola, Y.H. Hu, Design and synthesis of 3D potassium-ion pre-intercalated graphene for supercapacitors, Ind. Eng. Chem. Res. 57 (2018) 3610–3616.
[31] L. Chang, Y.H. Hu, Highly conductive porous Na-embedded carbon nanowalls for high-performance capacitive deionization, J. Phys. Chem. Solids 116 (2018) 347–352.
[32] L. Chang, Y.H. Hu, Surface-microporous graphene for high-performance capacitive deionization under ultralow saline concentration, J Chem. Phys. Solids 125 (2018) 135–140.
[33] L. Chang, Y.H. Hu, 3D channel-structured graphene as efficient electrodes for capacitive deionization, J. Colloid Interface Sci. 538 (2019) 420–425.
[34] L. Chang, Y.H. Hu, New chemistry for new material: highly dense meso-porous carbon electrode for supercapacitors with high areal capacitance, ACS Appl. Mater. Interfaces 10 (2018) 33162–33169.
[35] Z.U. Khan, T. Yan, L. Shi, D. Zhang, Improved capacitive deionization by using 3D intercalated graphene sheet-sphere nanocomposite architectures, Environ. Sci.: Nano 5 (2018) 980–991.
[36] M. Naebe, J. Wang, A. Amini, H. Khayyam, N. Hameed, L.H. Li, Y. Chen, B. Fox, Mechanical property and structure of covalent functionalized graphene/epoxy nanocomposites, Sci. Rep. 4 (2014) 4375.